

# Fermi 130 GeV gamma-ray excess and dark matter annihilation in sub-haloes and in the Galactic centre

Elmo Tempel<sup>a,b</sup>, Andi Hektor<sup>a</sup> and Martti Raidal<sup>a,c,d</sup>

(a) NICPB, Ravala 10, Tallinn 10143, Estonia

(b) Tartu Observatory, Observatooriumi 1, Tõravere 61602, Estonia

(c) Institute of Physics, University of Tartu, Estonia

(d) CERN, Theory Division, CH-1211 Geneva 23, Switzerland

## ABSTRACT

We analyze publicly available Fermi-LAT high-energy gamma-ray data and confirm the existence of clear spectral feature peaked at  $E_\gamma = 130$  GeV. Scanning over the Galaxy we identify several disconnected regions where the observed excess originates from. Our best optimized fit is obtained for the central region of Galaxy with a clear peak at 130 GeV with statistical significance  $4.5\sigma$ , while for the other regions the peak significances vary between  $3.2\sigma$  and  $1.6\sigma$ . The observed excess is not correlated with Fermi bubbles. We compute the photon spectra induced by dark matter annihilations into two and four standard model particles, the latter via two light intermediate states, and fit the spectra with data. Since our fits indicate sharper and higher signal peak than in the previous works, data disfavours all but the dark matter direct two-body annihilation channels into photons. Due to the final state radiation our fits prefer dark matter mass 145 GeV for the  $\gamma\gamma$  channel. We obtain large gamma-ray fluxes from Galactic centre that imply large annihilation cross-sections of order thermal freeze-out cross-section, if the Einasto halo profile correctly predicts the central cusp. If the observed gamma-ray excess comes from dark matter annihilations, we have identified the most dense dark matter sub-structures of our Galaxy. The large dark matter two-body annihilation cross-section to photons may signal a new resonance that should be searched for at the CERN LHC experiments.

May 2012

# 1 Introduction

If the existing cosmological dark matter (DM) [1] is a thermal relic consisting of weakly interacting massive particles, DM annihilations into the standard model (SM) particles should provide indirect evidence of DM in cosmic ray experiments [2]. In this scenario the first emerging signal of DM annihilations is expected to appear from Galactic regions with the highest DM density such as the centre of Galaxy or the largest DM sub-haloes. Very recently it was claimed [3, 4] that there is a  $4.6\sigma$  ( $3.3\sigma$ ) local (global) evidence of a monochromatic gamma-ray line [5, 6] with an energy  $E_\gamma \approx 130$  GeV present in the Fermi Large Area Telescope (LAT) [7] publicly available data. The signal originates from the centre of Galaxy from a region obtained applying a signal-to-background optimization procedure on the gamma-ray data [4]. If the claim is true, this could be the very first evidence that the DM is of particle physics origin, representing a breakthrough both in cosmology and in particle physics.

According to the analyses presented in Ref. [4], fitting the Fermi-LAT excess with a narrow peak is more an assumption rather than a result. In fact, any sufficiently hard spectrum with sharp fall-off around 130 GeV, for example a box, would fit the data presented in Fig. 4 of [4] as well as the narrow peak [8]. This would open a possibility to explain the excess with astrophysical sources, for example with an unknown mechanism associated with the Fermi bubbles [9, 10]. As the best signal-to-background regions determined in [4] seem to overlap with the Fermi bubbles, such a qualitative connection is easy to come. In addition, this would also allow to explain the observed excess with photon spectra from DM annihilations into standard model final states that produce significant amount of prompt photons in their decays [11]. Discriminating between those possibilities requires thorough study of the Fermi data.

In this work we analyze the publicly available Fermi-LAT gamma-ray data in order to check and study independently the claim of  $E_\gamma \approx 130$  GeV excess. We analyze the Fermi-LAT 195 week ULTRACLEAN dataset using the kernel smoothing method for fitting that is independent of binning and is complementary to the sliding energy window method used by Weniger. We estimate the errors of our fits with the bootstrap method. We are interested in finding out whether the excess exists, what is its spatial distribution in the Galaxy, what is its spectrum, possible origin etc.

Fitting the photon spectrum coming from the regions identified by Weniger, we do confirm the existence a spectral feature in the analyzed data centered at  $E_\gamma = 130$  GeV. Knowing the energy of excess, we scan the data to find the regions where the excess comes from. We find that the excess originates from relatively small disconnected regions, the most important of them is the centre of Galaxy but several other regions exist. Away from the identified regions the excess disappears consistently with the expectations from DM annihilations. We fit the gamma-ray background at energies 20-300 GeV from data by cutting out the central signal region of the Galaxy. We obtain a perfect power-law fit with a power 2.6 for the high-energy gamma-ray background. We then fit the spectrum from the central signal region and observe a clear peak at  $E_\gamma \approx 130$  GeV with a local statistical significance  $4.5\sigma$ . Fits from other regions have significances between  $3.2\sigma$  and  $1.6\sigma$ . Our results indicate that the shape of the peak is even more pronounced than obtained in [4] – we observe also a rise of the peak. This result disfavors

any possible explanation to the observed excess with shallow spectra (including the box-like spectra) over the power-law background, and favours more peaky profiles that may be difficult to obtain from standard astrophysical sources. We study, classify and fit the possible model independent DM annihilation scenarios [12] into two and four standard model final states (the latter is assumed to occur via light intermediate states [13] that may also induce Sommerfeld enhancement of the annihilation cross-section). We find that our results disfavour any other scenario but direct two-body annihilation to photons. Due to the final state radiation, our fit prefers dark matter mass 145 GeV for the  $\gamma\gamma$  annihilation channel. Due to large gamma-ray fluxes from our signal regions the DM annihilation cross-section must be of order thermal freeze-out cross-section. This result depends very sensitively on the unknown properties of the central cusp of our Galaxy and can therefore be relaxed. Increasing the loop-suppressed DM annihilation cross-section to photons may require the existence of new resonances that should be searched for at the CERN LHC experiments.

An important result of Ref. [4] is showing that regions with optimal size should be used for this type of search – likely the reason why Fermi Collaboration did not observe the excess is that they looked at too large region [14]. However, we do not see any reason why the low energy gamma-ray spectrum at energies  $1 \text{ GeV} < E_\gamma < 20 \text{ GeV}$  should be used to identify the best signal regions above  $E_\gamma > 100 \text{ GeV}$ . To the contrary, we believe that using the low energy spectrum for these purposes may be misleading. For example, we observe a slight asymmetry in the low energy spectrum that explains the north-south asymmetry of the identified regions in [4]. Since for large regions the background is completely dominated by the Galactic disk, the requirement of good signal-to-background ratio cuts off the disk region. Thus the shape of the regions obtained in [4] must trivially be of a hourglass type – their overlap with the Fermi bubbles is most likely accidental. This coincidence lead some authors to speculate that the signal is associated with Fermi bubbles while the photons from the centre follow power-law background [10]. Our results show that the actual situation with the  $E_\gamma = 130 \text{ GeV}$  excess is exactly opposite and the observed signal cannot be associated with the Fermi bubbles.

Based on that criticism we search for signal regions and optimize their size ourselves. We find that the optimal signal region for the best statistical significance is covered by the radius of  $3^\circ$  in the Galactic centre. For larger regions the signal significance decreases due to larger background, for smaller regions, like the Reg 5 in [4], the signal decreases because of too small number signal photons from that small region. Thus we confirm the necessity of right choice of the signal regions. Our results show that the peak excess is concentrated to rather small regions. If the source of the 130 GeV photons is astrophysical, further investigation of those regions with different observation frequencies should reveal objects or processes that also produce the 130 GeV gamma-rays. However, if the origin of the excess is direct DM annihilation into photons, we may have identified the first DM sub-haloes of our Galaxy.

## 2 Data analyses

### 2.1 Data selection

In the present analysis, we take into account 195 week of data from the Fermi Large Area Telescope (LAT) (from 4 Aug 2008 to 18 April 2012) with energies between 20 and 300 GeV. We apply the zenith-angle cut  $\theta < 100^\circ$  in order to avoid contamination with the earth albedo, as recommended by the Fermi LAT team. We also apply the recommended quality-filter cut DATA\_QUAL= 1, LAT\_CONFIG= 1, and ABS(ROCK\_ANGLE)< 52. We make use of the ULTRACLEAN events selection (Pass 7 Version 6), in order to minimise potential statistical errors. The selection of events as well as the calculation of exposure maps is performed using the 18 April 2012 version of ScienceTools v9r27p1. For everything else we use our own software.

### 2.2 Spectra estimation

Calculating the spectra from observed events is practically a probability distribution estimation. Estimating probability distributions is a well-developed topics in statistics, and we can choose all the modern tools – kernel densities, adaptive kernels, smoothed bootstrap for point-wise confidence intervals. In [15] this method is applied to study the luminosity function of galaxies. In this paper we shall use the same method, briefly reviewed below.

The simplest approach to find a observed spectra is the binned density histogram that depends both on the bin widths and the location of the bin edges. A better way to estimate a probability distribution is to use kernel smoothing (see, e.g. [16]), where the density is represented by a sum of kernels centred at the data points:

$$\Phi(E) = \sum_i \frac{1}{h_i} K\left(\frac{E - E_i}{h_i}\right). \quad (1)$$

The kernels  $K(x)$  are distributions ( $K(x) > 0$ ,  $\int K(x)dx = 1$ ) of zero mean and of a typical width  $h$ . The width is an analogue of the bin width, but there are no bin edges to worry about. In the latter equation, we use the adaptive kernel estimation, where the kernel widths depend on the data,  $h_i = h(E_i)$ . The summation is taken over all data points (events).

The kernel widths are known to depend on the density  $f(x)$  itself, with  $h \sim f(x)^{-0.2}$  (see, e.g. [17]): in regions of fewer data points, we use wider kernels. This choice requests a pilot estimate for the density that can be found using a wide constant width kernel.

To estimate the spectra, we use  $B_3$  box spline kernel:

$$B_3(x) = \frac{|x - 2|^3 - 4|x - 1|^3 + 6|x|^3 - 4|x + 1|^3 + |x + 2|^3}{12}. \quad (2)$$

This kernel is well suited for estimating densities – it is compact, differing from zero only in the interval  $x \in [-2, 2]$ , and it conserves mass:  $\sum_i B_3(x - i) = 1$  for any  $x$ . This kernel is also close to Gaussian with  $\sigma = 0.6$ .

We used the logarithmic energy scale for our spectra estimation. For the pilot estimate, we used a wide kernel with the scale  $h = 0.1$  (in logarithmic energy scale). For the adaptive kernel widths, we adopted  $h = 0.03$  (the typical uncertainties in the overall energy calibration of the Fermi LAT) as the minimal width (for the maximum pilot density) and rescaled it by the  $h \sim f_{\text{pilot}}(x)^{-0.2}$  law. The event probability drops rapidly at the high energies, leading to very wide kernels; we restricted the maximum kernel with by  $h = 0.1$ .

If we choose the kernel width this way, we minimize the mean integrated standard error (MISE) of the density. We are also interested in the “error bars”, point-wise confidence limits (CL) for the density. This can be obtained by smoothed bootstrap ([18]; [19]). Here the data points for the bootstrap realizations are chosen, as usual, randomly from the observed data with replacement, but they have an additional smoothing component:

$$E_i^* = E_j + h\epsilon_j, \quad (3)$$

where  $\epsilon$  is a random variable of the density  $K(x)$ .

We generated 10000 bootstrap realizations, using the adaptive kernel widths. We show the centered 95% confidence regions in our figures.

Using the kernel smoothing method to estimate the probability distribution is appropriate when the potential signal is weak or the number of data points is small. In this case the usual binning technique may hide the signal or introduce a false signal, depending on the bin width and bin location. The kernel smoothing method depends only on the number of data points and the used kernel widths. Whereby, the kernel widths take into account the uncertainties of the observed data points and this way the resulting distribution function is effectively unaffected of it. As a result, the estimated probability distribution reveals the true observed distribution as accurately as possible.

### 3 Fits to data: signal versus background

Our aim is to perform as model independent fits to the Fermi LAT data as possible. To achieve this goal we first find the high-energy gamma-ray background from data. For that we exclude the central Galactic region with a radius of  $12^\circ$  from data and fit all the data in the energy range  $20 \text{ GeV} < E_\gamma < 300 \text{ GeV}$ . The choice to exclude the central region of Galaxy from the background fit is motivated by the expected signal in this region. However, actually the result is insensitive to doing that. The fitting procedure is described in the previous section. We obtain almost perfect power-law background estimate from data with the power 2.6. This result agrees well with theoretical expectations and shows that the gamma-ray background in this energy region is induced by scattering of high-energy diffuse protons. We use the data-fitted background in all our computations.

Logically the first step towards more thorough analyses is to check the claim of the existence of  $E_\gamma = 130 \text{ GeV}$  spectral feature in the data. For that we first choose the Reg3 identified in Ref. [4] as our signal region and fit the gamma-ray data from that region as described in the previous

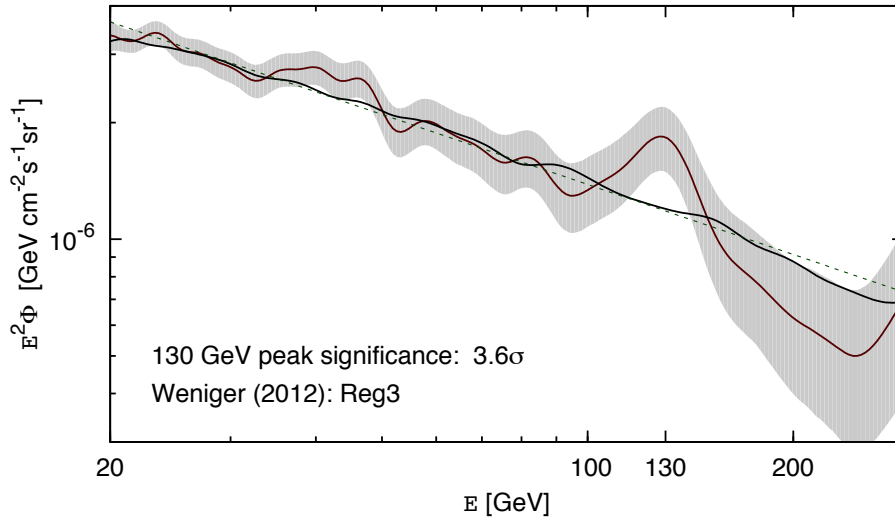


Figure 1: *Estimated high-energy gamma-ray spectrum originating from Reg 3 of Ref. [4] together with 95% CL error band as a function of photon energy. Data fitted background is also shown, the power-law spectrum with power 2.6 is plotted for comparison.*

section. The result is shown in Fig. 1 where we plot the resulting gamma-ray spectrum (red solid line) as a function of photon energy for the high-energy region  $20 \text{ GeV} < E_\gamma < 300 \text{ GeV}$ . The 95% CL error band is shown with a grey band around the best fit. The background obtained from data (black solid line) and the perfect power-law spectrum with power 2.6 (dashed line) are also shown. The total number of high-energy photons and the number of photons with energies  $120 \text{ GeV} < E_\gamma < 140 \text{ GeV}$  coming from this signal region are presented in Table 1. The excess at  $E_\gamma = 130 \text{ GeV}$  with statistical significance  $3.6\sigma$  is clearly visible. We observe that the excess has a more pronounced peak-like shape than that presented in Fig. 4 of Ref. [4]. However, the overall flux we obtain is in good agreement with the gamma-ray flux obtained in Ref. [4].

Having confirmed the previous claims, the next question to ask is from which region of the Galaxy the photons in the peak come from? For illustration of data we first plot the distribution of photons in the energy range  $120 \text{ GeV} < E_\gamma < 140 \text{ GeV}$ , denoted with blue dots, in the left panel of Fig. 2. Thus the figure is actually a Fermi photograph of our Galaxy in this energy range. As expected, we observe that most of the photons in that energy range come either from the very centre of the Galaxy or from the Galactic disk area.

In order to find the spatial origin of the excess we scan over the Galaxy choosing circle regions with varying radii in different locations and fitting data coming from those regions as described before. Looking for the maximal statistical significance of the 130 GeV signal we identify both the location as well as the optimal size of the signal regions. We define the intensity of the signal as follows. We compute the deviation of the ratio of observed spectrum over the background spectrum at  $E_\gamma = 130 \text{ GeV}$ ,  $\Delta_\gamma = (f^{obs}/f^{bkg} - 1)$ , and multiply this with the number of photons with energies  $120 \text{ GeV} < E_\gamma < 140 \text{ GeV}$  from this region. In this way the quantity  $N \cdot \Delta_\gamma$ ,

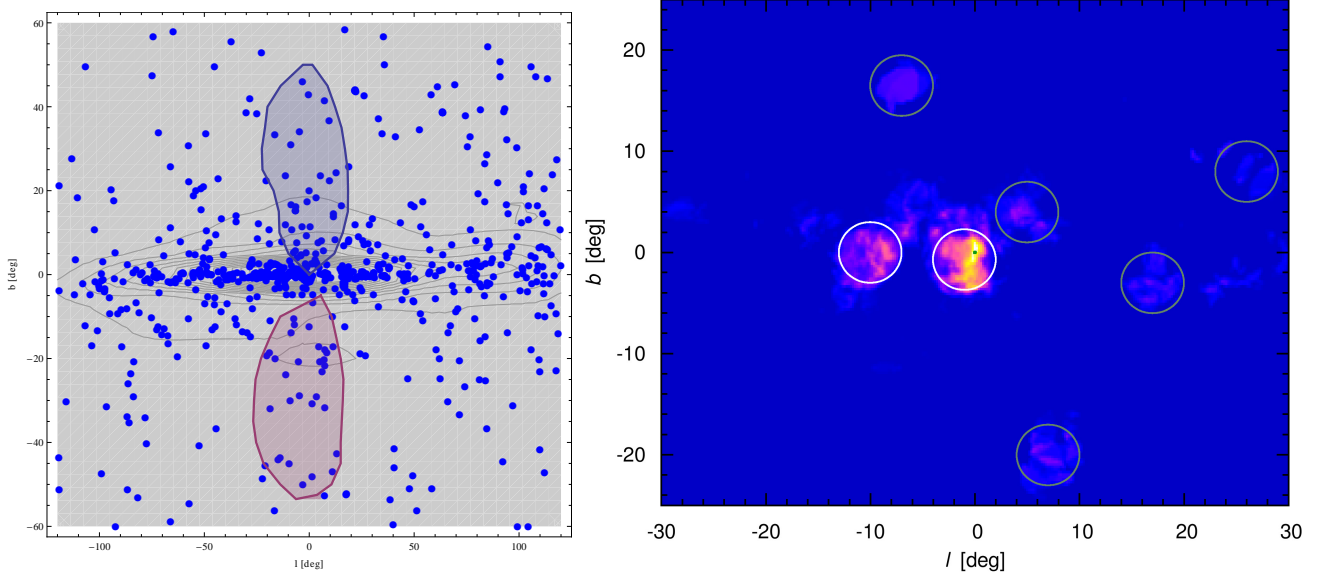


Figure 2: *Left: a Fermi “photograph” of our Galaxy in gamma-rays with the energy  $120 \text{ GeV} < E_\gamma < 140 \text{ GeV}$ . Fermi data is shown with blue dots. Fermi bubbles are also shown for illustration. Right: intensity of the  $120 \text{ GeV} < E_\gamma < 140 \text{ GeV}$  photons in the Galaxy. The white circles denote the signal regions that provide the excess with highest statistical significance; grey circles denote other regions showed in Table 1; green dot mark the assumed centre of the Galaxy.*

the signal intensity, takes into account both the height of the peak and the number of photons from the signal region.

We plot in the right panel of Fig. 2 the resulting signal intensity in the Galaxy. As seen in the figure, the most intense signal originates from the centre of Galaxy. This region is centered at  $(l, b) = (-1^\circ, -0.7^\circ)$ , called “Central” region in the following, and has a radius  $\sim 3^\circ$ , drawn with a white circle in Fig. 2. The total number of high-energy photons and the number of  $120 \text{ GeV} < E_\gamma < 140 \text{ GeV}$  photons coming from this signal region is presented in Table 1. However, there exist other regions, spatially well separated from the centre, that also exhibit large  $130 \text{ GeV}$  gamma-ray excess over the background. The most intense of them, with the same radius, is located at  $(l, b) = (-10^\circ, 0^\circ)$ , called “West” region in the following, and is also shown in the figure. The remaining bright signal regions are all listed in Table 1. Presently statistically significant fits are obtained only for the first two-three regions, but with more Fermi statistics the other regions may become relevant too.

It is clear from Fig. 2 that the excess of photons with energy around  $130 \text{ GeV}$  does not originate from Fermi bubbles. Firstly, there is no spatial correlation between the signal intensity and the Fermi bubbles. Secondly, whatever is the physical mechanism creating the  $130 \text{ GeV}$  excess, this mechanism must be at work in several regions of the Galaxy. If the origin of the excess is astrophysical, it should be possible to observe those astrophysical objects/processes in the identified regions with other methods. Any such a mechanism must also explain why the

Table 1: Identified signal regions in the Galaxy, number of photons in the two energy intervals and the statistical significance of excess in those regions. The radii of regions are all  $3^\circ$ .

Region	l (deg)	b (deg)	$N_\gamma$ (20-300) GeV	$N_\gamma$ (120-140 GeV)	significance
Weniger Reg3	-	-	3298	65	$3.6\sigma$
Central	-1	-0.7	818	27	$4.5\sigma$
West	-10	0	726	21	$3.2\sigma$
East	17	-3	462	14	$2.7\sigma$
South	7	-20	58	6	$2.5\sigma$
North-East 1	26	8	104	4	$2.0\sigma$
Noth-East 2	5	4	224	6	$1.8\sigma$
North	-7	16.5	110	4	$1.6\sigma$

observed excess is a peak, that might be difficult in the case of standard astrophysical processes. If, however, the origin of the 130 GeV peak is DM annihilations, Fig. 2 shows the distribution of the most dense DM sub-haloes in the central region of our Galaxy. Notice that the dark centre of the Galaxy does not exactly coincide with the galactic coordinate origin.

The fits to high-energy gamma-ray data originating from the Central and West signal regions are plotted in the left and right panels of Fig. 3, respectively, using the same notation as in Fig. 1. The Central region exhibits an excess with statistical significance of  $4.5\sigma$ . However, also the fit to West region shows a clear peak at 130 GeV with statistical significance of  $3.2\sigma$ . We have also fitted the signal from other bright regions in Fig. 2 that all show an excess peaked at the same photon energy,  $E_\gamma = 130$  GeV. Those are listed in Table 1. However, notice that the magnitude of the gamma-ray flux we obtain from those signal regions is larger than the flux presented in Fig. 1.

Based on the model independent results presented in Figs. 1-3 and in Table 1, we conclude that, whatever is the physics origin of the excess, its significance is high, it has a clear peak shape, and it comes from several regions around the Galactic centre.

## 4 Fitting DM annihilation spectra

### 4.1 Comparison of different annihilation channels

It is appealing to attempt to explain that the observed gamma-ray excess with DM annihilations in the Galactic centre and in the most dense DM sub-haloes around the centre of our Galaxy. Our approach is model independent as described in Refs. [2, 12]. We assume that the DM particles annihilate into two SM particles,  $DM + DM \rightarrow SM + SM$ , where  $SM = \gamma, e, \mu, \tau, q, W, Z, h$ , where  $q$  denotes any light or heavy quark. The final state SM particles decay and/or radiate photons and light fermions from the final state radiation. In addition,



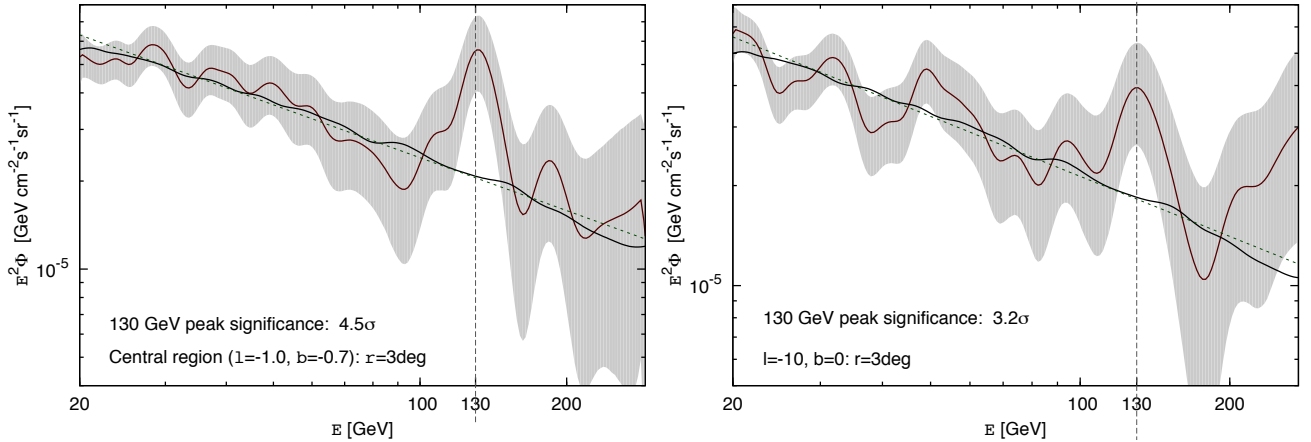


Figure 3: *Best fits to high-energy gamma-ray data for the Central (left panel) and West (right panel) signal regions presented in Table 1, together with 95% CL error band as functions of photon energy. Background fitted from data is also shown, the power-law spectrum with power 2.6 is plotted for comparison.*

we also allow DM annihilations into two light hypothetical final states,  $DM + DM \rightarrow V + V$ , that decay as  $V \rightarrow \gamma\gamma, ee, \mu\mu$ . Those particles have been postulated to exist [13] in order to explain the DM annihilations to lepton and not quark final states. In addition, those light particles may induce Sommerfeld enhancement of the annihilation cross-section. Both those features are needed to explain the PAMELA anomaly of positron flux with DM annihilation scenarios. Assuming those annihilation channels we have computed the resulting decay/hadronization chains and final state radiation with PYTHIA [20], and obtained the resulting prompt photon spectra. We use those prompt spectra to fit the observed gamma-ray excess. We neglect photons from inverse Compton scatterings between possible charged annihilation products and the Galactic and CMB background photons as this spectrum is too distributed to explain the observed peaked excess.

To study which DM annihilation scenarios can explain the observed excess best we estimate the goodness of the fit as follows. To fit the peak we choose the signal energy range to be  $50 \text{ GeV} < E_\gamma < 200 \text{ GeV}$  and divide it into  $n = 100$  bins. We compute  $\chi^2$  according to

$$\chi^2 = \sum_i^n \frac{(f_i^{th} - f_i^{obs})^2}{\sigma_i^{obs2}}, \quad (4)$$

where  $f_i^{obs}$  and  $\sigma_i^{obs}$  are the observed flux and its error from our fits to data for a bin  $i$ , and  $f_i^{th}$  is a theory estimate of signal plus background computed for every annihilation channel. The theoretical spectrum is calculated the same way as observed spectrum (see Sect. 2.2) to have comparable spectra. For every annihilation channel we find the minimal reduced  $\chi^2/n$  that gives the best fit of that theoretical model to data.

Contrary to our initial intuition based on Ref. [4] results, almost all the resulting photon spectra from DM annihilations turn out to be too soft to explain the observed gamma-ray excess. Our

best fit (for the Central signal region) for the annihilation channel  $DM + DM \rightarrow \gamma + \gamma$ , denoted by blue dotted line, is presented in the left panel of Fig. 4 together with the fit to data as in Fig. 3. The best fit  $\chi^2/n = 0.9$  is obtained for the DM mass  $M_{DM} = 145$  GeV. It was shown in Ref. [4] that DM annihilations into a monochromatic gamma-ray line can fit the data. The main difference between our result compared to Ref. [4] is that our photon spectrum is *realistic* not an assumed peak. The assumed 130 GeV peak is also shown in this Figure. The prompt photons produced in DM annihilation with so large energy radiate light fermion pairs and lose energy quite effectively. Therefore the peak moves from 145 GeV to lower energies and the resulting photon spectrum from the  $\gamma\gamma$  final state is actually broader than naively expected. For comparison we also present in the same plot the monochromatic gamma line that would arise from 130 GeV DM annihilation into two photons if there was no final state radiation. This is presented in the figure by green dotted line. It gives  $\chi^2/n = 0.4$ , indicating overfitting. Clearly, for  $M_{DM} = 145$  GeV, the  $\gamma\gamma$  channel gives a good fit to the observed 130 GeV gamma-ray peak.

The second hardest photon spectrum is obtained for  $DM + DM \rightarrow V + V \rightarrow 4\gamma$  channel, all the remaining studied channels produce so broad photon spectrum that cannot fit the observed peak. We present the best fit for this channel with  $\chi^2/n = 1.9$  in the right panel of Fig. 4 for the same DM mass  $M_{DM} = 145$  GeV. This annihilation channel can reproduce the fall-off of the peak but predicts flat box-like distribution for smaller than the peak energies. The reduced  $\chi^2/n$  is 1.9 compared with 0.9 for the  $2\gamma$  channel and the fit is clearly worse. It is still possible that, due to limited statistics, we observe significant down-ward fluctuation at photon energies  $\sim 100$  GeV. With the present statistics the probability this to happen is at the level of a few percent. Examples of such fluctuations are presented in the right panel of Fig. 4 with green dotted lines. If we observe the down-ward fluctuation, this should disappear with more data and the observed peak will be replaced by a box-like spectrum. This scenario looks, however, unlikely.

## 4.2 Fitting annihilation cross-section

Up to now we have made no assumption about the DM distribution in the main DM halo of the Galaxy. However, if we want to estimate the annihilation cross-sections that fit the signal, we must compute the absolute flux of gamma-rays coming from the signal regions. Here we work only with the Central signal region. We assume two different halo profiles, the Einasto profile [21, 22, 23, 24],

$$\rho_{\text{Ein}}(r) = \rho_s \exp \left\{ -\frac{2}{\alpha} \left[ \left( \frac{r}{r_s} \right)^\alpha - 1 \right] \right\}, \quad (5)$$

with  $\alpha = 0.17$ ,  $\rho_s = 0.079$ , and  $r_s = 20$  and the Navarro-Frenk-White (NFW) profile [25, 14],

$$\rho_{\text{NFW}}(r) = \rho_s \frac{r_s}{r} \left( 1 + \frac{r}{r_s} \right)^{-2}, \quad (6)$$

with  $\rho_s = 0.33$  and  $r_s = 20$ . The profiles have been normalized to the local DM density  $\rho_{\text{DM}} = 0.4$  GeV cm $^{-3}$  at the Solar system [26, 27]. The gamma-ray flux from Central signal

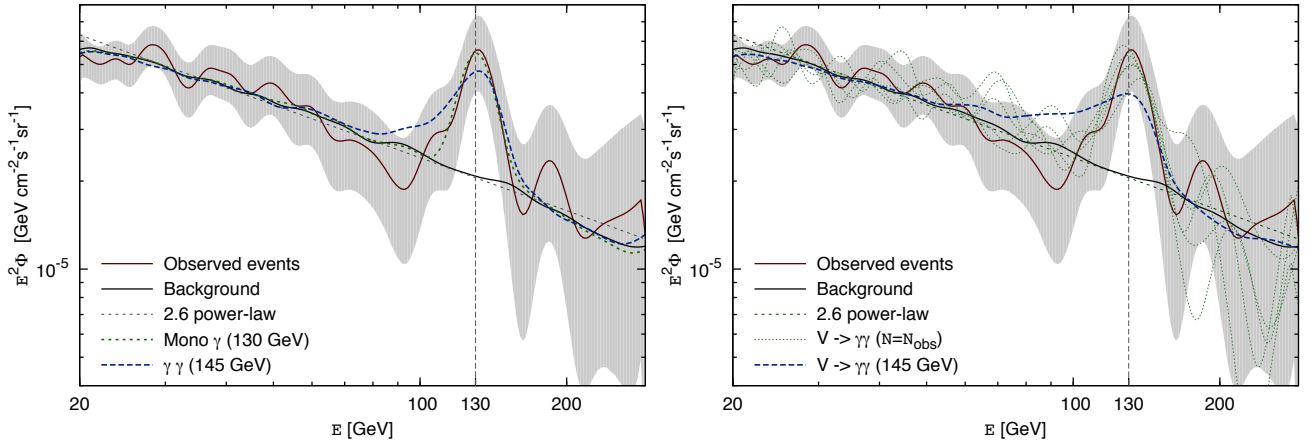


Figure 4: *Best fit to data from the Central region with DM annihilation spectra into  $2\gamma$  (left panel) and to  $2V \rightarrow 4\gamma$  (right panel), presented with dashed blue lines, for DM mass  $M_{DM} = 145$  GeV. The rest is as in Fig. 3. The latter case can fit data only if large statistical fluctuation of the spectrum occur due to the present limited statistics, as demonstrated in the right panel with green dotted lines.*

region is calculated according to formalism presented in [2]. To estimate the annihilation cross-section,  $\langle\sigma v\rangle$ , we let it to vary and compute the corresponding  $\chi^2/n$  of the flux according to eq. (4). The minimal  $\chi^2/n$  gives the best fit value for  $\langle\sigma v\rangle$ . The  $1\sigma$  errors to the cross-sections are estimated by requiring  $\Delta(\chi^2/n) = 1$ .

The results for  $2DM \rightarrow 2\gamma$  and  $2DM \rightarrow 2V \rightarrow 4\gamma$  annihilation channels are presented in Table 2. They correspond to the cases plotted in Fig. 4. The cross-sections are required to be very large, of order of standard thermal cross-sections. This is about one order of magnitude larger than the result obtained by Weniger. The reason for such an increase is twofold. Firstly, the flux that we obtain is much higher than the one obtained by Weniger as is clearly seen by comparisons of fluxes in Fig. 1 and in Fig. 4. Also the peak we obtain is much more pronounced than that in Ref. [4]. Higher flux implies larger annihilation cross-section. Secondly, since we take into account the final state radiation, significant fraction of energy in the photon flux is “lost” due to creation of fermion pairs. This has an effect of increasing the DM mass and, to compensate the losses, also increasing the annihilation cross-section.

Notice that the errors in estimating the cross-sections are huge. This is because we fit the peak and the overall  $\chi^2$  fit is not very sensitive to that. But qualitatively our results do favour large annihilation cross-section. Those can be explained by cross-section enhancement mechanisms like the Sommerfeld enhancement or resonances in the annihilation process. We will elaborate on the latter in the next section. The enhancement of the flux can also be explained by nonstandard DM cusp in the centre of Galaxy. In this case the annihilation cross-section can be small with the price of making the central cusp DM density bigger than predicted by the profiles we assume. If the main halo has substructures in the central region as favoured by our results the presented cross-sections can have larger uncertainties as presented

Table 2: The annihilation cross-sections given in units of the standard thermal cross-section,  $\langle\sigma v\rangle = 3 \times 10^{-26} \text{ cm}^3 \text{ s}^{-1}$  together with  $1\sigma$  errors.

Channel	$\langle\sigma v\rangle$ for Einasto	$\langle\sigma v\rangle$ for NFW
$2DM \rightarrow 2\gamma$	$1.48^{+1.36}_{-0.87}$	$2.84^{+2.63}_{-1.66}$
$2DM \rightarrow 2V \rightarrow 4\gamma$	$0.47^{+0.41}_{-0.28}$	$0.9^{+0.79}_{-0.54}$
Idealistic monochromatic $2\gamma$	$0.30^{+0.27}_{-0.17}$	$0.58^{+0.52}_{-0.33}$

here. Probably, the over-dense substructures can explain the enchantment of the cross-sections over the standard thermal value.

## 5 Discussion of the results

While we do confirm the existence of the 130 GeV excess in Fermi LAT data, our results differ from the ones presented by Ref. [4] in some important aspects. Firstly, our search strategy for finding the most sensitive signal regions in the Galaxy gives significantly different results than obtained by Weniger. We do not see any reason why one should use the low energy data,  $1 \text{ GeV} < E_\gamma < 20 \text{ GeV}$ , to determine the high-energy background. At such low energies the background may be distorted by astrophysical sources like Fermi bubbles and, indeed, we observe north-south asymmetry in the low energy data. This explains why the Weniger regions are asymmetric. In addition, Weniger’s signal regions similarity with Fermi bubbles is most likely accidental but misleading. At the end, the fit to data from those regions gives quite significant excess, see Fig. 1. Instead, we fitted the background from high-energy data by excluding the centre of Galaxy and searched for the 130 GeV signal regions by scanning the data. With this procedure we identified small regions where the signal significantly exceeds the background, presented in Fig. 2 and Table 1. In the context of our approach, those may correspond to DM sub-haloes of our Galaxy.

Secondly, our results show that the excess has clearly a shape of the peak while Weniger’s data analyses may also be consistent with a box-like excess. This result narrows the possible astrophysical explanations to the excess. This result also disfavours all DM annihilation modes but the direct one to photons (internal bremsstrahlung [28, 29, 30] spectrum is likely also allowed), which, as we have shown, are not so monochromatic at those energies. In addition, we find that energy loss due to final state radiation in the  $\gamma\gamma$  final state increases the DM mass to 145 GeV.

We find that the effect of final state radiation and the largeness of the gamma-ray flux from the Central signal region require the DM annihilation cross-section  $\langle\sigma v\rangle$  to be as large as the thermal freeze-out cross-section, although the errors are very large. There are two possible ways to explain this result. Firstly, the DM annihilation cross-section into  $\gamma\gamma$  may be small, but the DM halo models we have used, Einasto and NFW, fail to describe the central cusp

of our Galaxy. This is possible since N-body simulations cannot predict the central region precisely. Since the cross-section calculation depends on the halo properties, there is always large theoretical uncertainty related to that. Secondly, the annihilation cross-section into  $\gamma\gamma$  might be, indeed, enhanced. Thus the model building of DM theories should concentrate on  $\gamma\gamma$  or  $\gamma X$  annihilation modes and on the enhancement of those annihilation cross-sections to the observed level.

Generically one expects DM direct annihilation cross-section to photons to be orders of magnitude smaller than is needed to explain the observation. However, examples exist in which loop level [31, 32, 33, 34] or anomaly induced [35, 36] cross-sections to photons are enhanced. Motivated by the recent LHC results that at least one light fundamental scalar, the Higgs boson, likely exist with a mass 125 GeV, and no low scale supersymmetry nor Kaluza-Klein particles exist below 1 TeV, one can construct most plausible scenarios of thermal relic DM that have large annihilation cross-sections to  $2\gamma$  channel.

For example, one well motivated possibility is that the DM consists of dark scalars that couple to the SM fermion via extended Higgs sector with non-vanishing (or dominant) coupling only to the top quark. In this case the correct DM thermal relic abundance is induced via s-channel annihilation process for DM masses somewhat below the top quark mass. This is a generic prediction of the set-up not related to any model building detail but to the topology of freeze-out process and to the top mass. Today, when the DM is essentially at rest, the only kinematically allowed annihilation channel to the SM particles is opened by the top loop induced coupling to two photons (that dominates over the  $\gamma Z$ ,  $ZZ$  final states). This, as argued before, must be enhanced. The enhancement can occur due to an accidental resonance so that  $2M_{DM} \sim M_H$ , where  $M_H$  is the mass of new unobserved scalar. In this case all the parameters of the scenario are essentially fixed. The DM mass 145 GeV is consistent with thermal freeze-out, and new particle with non-standard couplings is predicted to exist with a mass  $M_H \sim 290$  GeV, depending somewhat on how close to the resonance the annihilation process must be. A drawback of the scenario is that the DM-nucleon scattering cross-section is predicted to be small, explaining the absence of signal in DM direct searches at XENON100 [37].

This scenario has already been realized in Ref. [34] for the  $\gamma h$  final state, where  $h$  is the SM Higgs boson, in the context of Randall-Sundrum framework with extra  $Z'$  boson. For the final states  $\gamma X$  the 130 GeV gamma-ray excess implies different DM mass that depends on the mass of  $X$  via  $E_\gamma = M_{DM}(1 - M_X^2/4M_{DM}^2)$ . Apart from the mass shift, to enhance the gamma-ray signal to the indicated level, all this type scenarios should include new resonance at  $2M_{DM}$  that can be searched for at the LHC experiments.

## 6 Conclusions

We have analyzed Fermi LAT publicly available data collected during 195 weeks and confirm the existence of gamma-ray excess peaked at  $E_\gamma = 130$  GeV. The excess originates from disconnected spatial regions, presented in Table 1. The excess is not correlated with Fermi bubbles.

The strongest signal over background comes from the central region of the Galaxy and has statistical significance of  $4.5\sigma$ , but the signal from the other regions shows also up to  $3\sigma$  excess. According to our fits the excess is narrower and higher than shown before. Leaving aside the possibility that the excess is an instrumental artifact, our results show that the mechanism of generating such an excess must be at work in several regions of our Galaxy. It might be difficult to explain the sharp gamma-ray peak with standard astrophysical processes. It is more appealing to assume that the excess originates from DM annihilations. In this case our results imply that we have identified the most dense DM substructures of our Galaxy – the central cusp and the largest DM sub-haloes.

Assuming the DM annihilation scenario, we have computed photon spectra from DM annihilations into two SM and into two light bosons  $V$  that decay to two photons or leptons using PYTHIA. We find that only the DM annihilations into  $\gamma\gamma$  channel with DM mass  $M_{DM} = 145$  GeV can fit data well. This is because prompt photons with so large energy radiate light fermions quite effectively and the resulting photon peak occurs at 130 GeV. All other spectra, including the  $4\gamma$  one from the intermediate  $V$  states, provide significantly worse fits to data. We obtain large gamma-ray flux from the Central signal region that imply that the DM annihilation cross-section into photons must be as high as the standard thermal freeze-out cross-section, with large errors. However, this result is correct only if the Einasto or NFW halo profiles predict the properties of the central cusp exactly. We have sketched a generic thermal relic DM scenario that, independently of model details, should produce the observed DM relic density and the enhanced DM annihilations into  $\gamma\gamma$  today. This scenario predicts a new resonance close to  $2M_{DM}$  with specific couplings that should be searched for at the LHC experiments. All the results above can be generalized to the DM annihilation channels into  $\gamma X$ , where  $X$  is any massive SM particle.

### Acknowledgement

We thank M. Cirelli, E. Gabrielli, C. Grojean, T. Hambye, G. Servant, A. Strumia and C. Weniger, for discussions and communications. This work was supported by the ESF grants 8090, 8499, 8943, MTT8, MTT59, MTT60, MJD140, MJD272, JD164, by the recurrent financing project SF0690030s09 and by the European Union through the European Regional Development Fund.

## References

- [1] E. Komatsu *et al.* [WMAP Collaboration], “Seven-Year Wilkinson Microwave Anisotropy Probe (WMAP) Observations: Cosmological Interpretation,” *Astrophys. J. Suppl.* **192** (2011) 18 [arXiv:1001.4538 [astro-ph.CO]].
- [2] For a review and for details of DM annihilation signals in cosmic ray spectra see, M. Cirelli, G. Corcella, A. Hektor, G. Hutsi, M. Kadastik, P. Panci, M. Raidal and F. Sala

- et al.*, “PPPC 4 DM ID: A Poor Particle Physicist Cookbook for Dark Matter Indirect Detection,” *JCAP* **1103** (2011) 051 [arXiv:1012.4515 [hep-ph]].
- [3] T. Bringmann, X. Huang, A. Ibarra, S. Vogl and C. Weniger, “Fermi LAT Search for Internal Bremsstrahlung Signatures from Dark Matter Annihilation,” arXiv:1203.1312 [hep-ph].
- [4] C. Weniger, “A Tentative Gamma-Ray Line from Dark Matter Annihilation at the Fermi Large Area Telescope,” arXiv:1204.2797 [hep-ph].
- [5] L. Bergstrom and H. Snellman, “Observable Monochromatic Photons From Cosmic Photino Annihilation,” *Phys. Rev. D* **37** (1988) 3737.
- [6] For complete set of references see,  
T. Bringmann, F. Calore, G. Vertongen and C. Weniger, “On the Relevance of Sharp Gamma-Ray Features for Indirect Dark Matter Searches,” *Phys. Rev. D* **84** (2011) 103525 [arXiv:1106.1874 [hep-ph]].
- [7] W. B. Atwood *et al.* [LAT Collaboration], “The Large Area Telescope on the Fermi Gamma-ray Space Telescope Mission,” *Astrophys. J.* **697** (2009) 1071 [arXiv:0902.1089 [astro-ph.IM]].
- [8] Private discussions with C. Weniger after CERN TH seminar in April 23, 2012.
- [9] M. Su, T. R. Slatyer and D. P. Finkbeiner, “Giant Gamma-ray Bubbles from Fermi-LAT: AGN Activity or Bipolar Galactic Wind?,” *Astrophys. J.* **724** (2010) 1044 [arXiv:1005.5480 [astro-ph.HE]].
- [10] S. Profumo and T. Linden, “Gamma-ray Lines in the Fermi Data: is it a Bubble?,” arXiv:1204.6047 [astro-ph.HE].
- [11] When our computations were finalized, this paper appeared that used similar idea to fit the gamma-ray excess with a box-like spectrum,  
A. Ibarra, S. Gehler and M. Pato, “Dark matter constraints from box-shaped gamma-ray features,” arXiv:1205.0007 [hep-ph].
- [12] M. Cirelli, M. Kadastik, M. Raidal and A. Strumia, “Model-independent implications of the  $e^+$ -, anti-proton cosmic ray spectra on properties of Dark Matter,” *Nucl. Phys. B* **813** (2009) 1 [arXiv:0809.2409 [hep-ph]].
- [13] N. Arkani-Hamed, D. P. Finkbeiner, T. R. Slatyer and N. Weiner, “A Theory of Dark Matter,” *Phys. Rev. D* **79** (2009) 015014 [arXiv:0810.0713 [hep-ph]].
- [14] A. A. Abdo, M. Ackermann, M. Ajello, W. B. Atwood, L. Baldini, J. Ballet, G. Barbiellini and D. Bastieri *et al.*, “Fermi LAT Search for Photon Lines from 30 to 200 GeV and Dark Matter Implications,” *Phys. Rev. Lett.* **104** (2010) 091302 [arXiv:1001.4836 [astro-ph.HE]].
- [15] E. Tempel, E. Saar, L. J. Liivamägi, A. Tamm, J. Einasto, M. Einasto and V. Müller, *Astronomy & Astrophysics* **529**, A53 (2011) [arXiv:1012.1470v2 [astro-ph.CO]].

- [16] M. P. Wand and M. C. Jones, Kernel Smoothing (Chapman & Hall) (1995).
- [17] B. W. Silverman, Density Estimation for Statistics and Data Analysis (Chapman & Hall) (1997).
- [18] A. C. Davison and D. V. Hinkley, Bootstrap Methods and their Application (Cambridge University Press) (1997).
- [19] C. V. Fiorio, The Stata Journal **4**, 168 (2004).
- [20] T. Sjostrand, S. Mrenna and P. Z. Skands, Comput. Phys. Commun. **178** (2008) 852 [arXiv:0710.3820 [hep-ph]].
- [21] J. Einasto, Trudy Inst. Astrofiz. Alma-Ata, 5 (1965) 87.
- [22] J. F. Navarro, E. Hayashi, C. Power, A. Jenkins, C. S. Frenk, S. D. M. White, V. Springel and J. Stadel *et al.*, “The Inner structure of Lambda-CDM halos 3: Universality and asymptotic slopes,” Mon. Not. Roy. Astron. Soc. **349** (2004) 1039 [astro-ph/0311231].
- [23] V. Springel, J. Wang, M. Vogelsberger, A. Ludlow, A. Jenkins, A. Helmi, J. F. Navarro and C. S. Frenk *et al.*, “The Aquarius Project: the subhalos of galactic halos,” Mon. Not. Roy. Astron. Soc. **391** (2008) 1685 [arXiv:0809.0898 [astro-ph]].
- [24] L. Pieri, J. Lavalle, G. Bertone and E. Branchini, “Implications of High-Resolution Simulations on Indirect Dark Matter Searches,” Phys. Rev. D **83** (2011) 023518 [arXiv:0908.0195 [astro-ph.HE]].
- [25] J. F. Navarro, C. S. Frenk and S. D. M. White, “A Universal density profile from hierarchical clustering,” Astrophys. J. **490** (1997) 493 [astro-ph/9611107].
- [26] R. Catena and P. Ullio, “A novel determination of the local dark matter density,” JCAP **1008** (2010) 004 [arXiv:0907.0018 [astro-ph.CO]].
- [27] P. Salucci, F. Nesti, G. Gentile and C. F. Martins, “The dark matter density at the Sun’s location,” Astron. Astrophys. **523** (2010) A83 [arXiv:1003.3101 [astro-ph.GA]].
- [28] J. F. Beacom, N. F. Bell and G. Bertone, “Gamma-ray constraint on Galactic positron production by MeV dark matter,” Phys. Rev. Lett. **94** (2005) 171301 [astro-ph/0409403].
- [29] L. Bergstrom, T. Bringmann, M. Eriksson and M. Gustafsson, “Gamma rays from Kaluza-Klein dark matter,” Phys. Rev. Lett. **94** (2005) 131301 [astro-ph/0410359].
- [30] L. Bergstrom, T. Bringmann, M. Eriksson and M. Gustafsson, “Gamma rays from heavy neutralino dark matter,” Phys. Rev. Lett. **95** (2005) 241301 [hep-ph/0507229].
- [31] M. Gustafsson, E. Lundstrom, L. Bergstrom and J. Edsjo, “Significant Gamma Lines from Inert Higgs Dark Matter,” Phys. Rev. Lett. **99** (2007) 041301 [astro-ph/0703512 [ASTRO-PH]].



- [32] J. Goodman, M. Ibe, A. Rajaraman, W. Shepherd, T. M. P. Tait and H. -B. Yu, “Gamma Ray Line Constraints on Effective Theories of Dark Matter,” Nucl. Phys. B **844** (2011) 55 [arXiv:1009.0008 [hep-ph]].
- [33] S. Profumo, L. Ubaldi and C. Wainwright, “Singlet Scalar Dark Matter: monochromatic gamma rays and metastable vacua,” Phys. Rev. D **82** (2010) 123514 [arXiv:1009.5377 [hep-ph]].
- [34] C. B. Jackson, G. Servant, G. Shaughnessy, T. M. P. Tait and M. Taoso, “Higgs in Space!,” JCAP **1004** (2010) 004 [arXiv:0912.0004 [hep-ph]].
- [35] E. Dudas, Y. Mambrini, S. Pokorski and A. Romagnoni, “(In)visible Z-prime and dark matter,” JHEP **0908** (2009) 014 [arXiv:0904.1745 [hep-ph]].
- [36] Y. Mambrini, “A Clear Dark Matter gamma ray line generated by the Green-Schwarz mechanism,” JCAP **0912** (2009) 005 [arXiv:0907.2918 [hep-ph]].
- [37] E. Aprile *et al.* [XENON100 Collaboration], “Dark Matter Results from 100 Live Days of XENON100 Data,” Phys. Rev. Lett. **107** (2011) 131302 [arXiv:1104.2549 [astro-ph.CO]].